

# RoCourseNet: Distributionally Robust Training of a Prediction Aware Recourse Model

Hangzhi Guo<sup>1</sup>, Feiran Jia<sup>1</sup>, Jinghui Chen<sup>1</sup>, Anna Squicciarini<sup>1</sup>, and Amulya Yadav<sup>1</sup>

<sup>1</sup>*College of Information Sciences and Technology, Pennsylvania State University*

## Abstract

Counterfactual (CF) explanations for machine learning (ML) models are preferred by end-users, as they explain the predictions of ML models by providing a recourse case to individuals who are adversely impacted by predicted outcomes. Existing CF explanation methods generate recourses under the assumption that the underlying target ML model remains stationary over time. However, due to commonly occurring distributional shifts in training data, ML models constantly get updated in practice, which might render previously generated recourses invalid and diminish end-users trust in our algorithmic framework. To address this problem, we propose RoCourseNet, a training framework that jointly optimizes for predictions and robust recourses to future data shifts. We have three main contributions: (i) We propose a novel *virtual data shift (VDS)* algorithm to find worst-case shifted ML models by explicitly considering the worst-case data shift in the training dataset. (ii) We leverage adversarial training to solve a novel tri-level optimization problem inside RoCourseNet, which simultaneously generates predictions and corresponding robust recourses. (iii) Finally, we evaluate RoCourseNet’s performance on three real-world datasets and show that RoCourseNet outperforms state-of-the-art baselines by  $\sim 10\%$  in generating robust CF explanations.

## 1 Introduction

Existing work in Explainable Artificial Intelligence (XAI) (Ribeiro et al., 2016; Lundberg and Lee, 2017; Koh and Liang, 2017; Wachter et al., 2017; Kim et al., 2018; Rudin, 2019) has been focused on developing techniques to interpret decisions made by black-box machine learning (ML) models. In particular, counterfactual (CF) explanation techniques (Wachter et al., 2017; Ustun et al., 2019; Mothilal et al., 2020; Karimi et al., 2021) are highly promising (and are often preferred by human end-users) because of their ability to provide actionable recourse<sup>1</sup> to individuals who are negatively impacted by algorithm-mediated decisions. For example, CF explanation techniques can be used to provide algorithmic recourse for impoverished loan applicants who have been denied a loan by a bank’s ML algorithm, or to provide recourse recommendations for school teachers working with students who are at the risk of dropping out from school, etc.

Unfortunately, most prior work on CF explanation techniques suffers from three major shortcomings. First, almost all existing techniques generate recourses by assuming that the underlying ML model is stationary and does not change over time (Barocas et al., 2020). However, in practice, ML models are often updated regularly when new data is available to improve predictive accuracy on the new shifted data distribution. This shifted ML model might render previously recommended recourses ineffective (Rawal et al., 2020), and in turn, diminish end users’ trust towards our system. Formally, when a shift occurs in the predictive model weights from  $\theta_f$  to  $\theta'_f$  (due to a shift in the underlying data distribution), a previously provided recourse  $x^{\text{cf}}$  generated based on  $\theta_f$  might become invalid on the shifted model weights  $\theta'_f$  (i.e.,  $f(x^{\text{cf}}; \theta_f) \neq f(x^{\text{cf}}; \theta'_f)$ ).

<sup>1</sup>Note that counterfactual explanation (Wachter et al., 2017), algorithmic recourse (Ustun et al., 2019), and contrastive explanation (Dhurandhar et al., 2018) are closely related (Verma et al., 2020; Stepin et al., 2021). Hence, we use these terms interchangeably.

This is undesirable to an end-user because in this situation, following recourse recommendations would not get them a favorable decision by the ML model.

Second, very limited prior work (Upadhyay et al., 2021) exists on generating robust CF explanations (against model shifts), but it suffers from two major drawbacks: (i) First, these methods locally approximate the underlying ML model with a linear model (e.g., LIME (Ribeiro et al., 2016)), which is then used as the target model to generate robust CF explanations. In addition to problems caused by the use of LIME (such as inconsistency (Slack et al., 2020) and unfaithfulness (Rudin, 2019)), it is inherently problematic to adopt local approximations of the ML model as the global target model. (ii) Second, they fail to explicitly consider the impact of shifts in the underlying data distribution, which is the fundamental reason causing model shifts in practice. Optimizing for robust CF explanations without considering data shifts could result in CF explanations which either require unnecessarily large changes to the input instance (i.e., they suffer from high proximity scores), or they are not robust against model shifts (as shown in Section 5).

Finally, existing techniques are post-hoc in nature, which are mainly designed for use with proprietary black-box ML models whose training data and model weights are not available. However, this black-box assumption is overly limiting in many real-world scenarios. With the advent of government regulations (like the EU-GDPR (Hoofnagle et al., 2019)), the same service provider (i.e., ML model designer) is often required to provide both their model’s prediction along with an explanation for that prediction. In these situations, it is sub-optimal for model designers to generate CF explanations (or recourse recommendations) by assuming black-box access to their ML model (since they have full access to their model internals and training data). In addition, the black-box assumption often leads to commonly faced issues of unfaithfulness and misalignment in post-hoc explanation methods (Rudin, 2019; Guo et al., 2021). Hence, it is desirable to develop CF explanation methods for situations when the predictive model is not black-box, and its model internals and training data can be fully accessed.

In this paper, we address these limitations by proposing RoCourseNet (*Robust ReCourse Neural Network*), an end-to-end training framework for simultaneously generating predictions and corresponding recourses (or CF explanations) that are robust to model shifts induced by distribution shifts in the training dataset. RoCourseNet addresses limitations of prior work via three key contributions:

- RoCourseNet is built on top of CounterNet (Guo et al., 2021), an end-to-end CF explanation framework (unlike post-hoc methods). This framework addresses the commonly faced misalignment issues in generating CF explanations by jointly optimizing predictions and corresponding CF examples.
- To train for robust CF generation, we leverage adversarial training to optimize a complicated tri-level (min-max-min) optimization problem. To optimize for the outer minimization problem, we adopt a block-wise coordinate descent procedure (Guo et al., 2021). Further, to optimize for the inner bi-level max-min problem, we devise a novel *Virtual Data Shift (VDS)* algorithm which finds an adversarially shifted model by explicitly simulating the *worst-case data shift* in the training set.
- Finally, we design rigorous experiments on three real-world datasets to evaluate the robustness of CF explanation methods under distributional shifts. Our results demonstrate that RoCourseNet generates highly robust CF explanations against data shifts as it consistently produces CF explanations with more than 91% robust validity, outperforming state-of-the-art baselines by  $\sim 10\%$ .

## 2 Related Work

**Counterfactual Explanation Techniques.** A significant body of literature exists on CF explanation techniques, which focuses on generating recourses that lead to different (and often more preferable) predicted outcomes (Wachter et al., 2017; Verma et al., 2020; Karimi et al., 2020). We categorize prior work on CF

techniques into *non-parametric methods* (Wachter et al., 2017; Ustun et al., 2019; Mothilal et al., 2020; Van Looveren and Klaise, 2019; Karimi et al., 2021; Upadhyay et al., 2021), which aim to find CF explanations without involving parameterized models, and *parametric methods* (Pawelczyk et al., 2020a; Yang et al., 2021; Mahajan et al., 2019; Guo et al., 2021), which adopt parametric models (e.g., a neural network model) to generate CF explanations. In particular, our work is most closely related to CounterNet (Guo et al., 2021), which unlike post-hoc methods, jointly trains the predictive model and a CF explanation generator. However, CounterNet does not optimize for the model shift problem, whereas we devise a novel adversarial training approach in RoCourseNet to ensure generating robust recourses.

**Robustness in Counterfactual Explanations.** We divide prior work on robustness of CF explanations into two categories: (i) ensuring robustness to small perturbations in the feature space of generated CF explanations; (ii) ensuring robustness to shifts in the target predictive model. In the first category, Pawelczyk et al. (2022) propose methods to ensure the validity of CF explanations when small perturbations in the feature space are added to them. Slack et al. (2020) introduce adversarial models to generate fundamentally different recourses with small perturbations to input instances.

In the second category, Pawelczyk et al. (2020b) introduce the *model multiplicity* problem which studies CF explanations’ validity under different ML models that are trained on the *same* data. On the other hand, Rawal et al. (2020) discuss the problem of *model shift*, which explores the scenario of shifting models due to distributional shifts in the training data. To tackle this problem, Upadhyay et al. (2021) propose ROAR, a post-hoc method which adopts adversarial training by perturbing the weights of the predictive model. However, ROAR is of limited utility because (i) it relies on a locally linear approximation (via LIME (Ribeiro et al., 2016)) to construct a shifted model, and (ii) it fails to explicitly consider the impact of data shifts. In contrast, our work addresses these limitations by explicitly considering data shifts for finding an adversarial model without demanding a local linear approximation.

**Adversarial training.** We also leverage techniques from the literature on adversarial robustness. It is well-known that adversarial training is effective in defending ML models against adversarial examples (Goodfellow et al., 2014; Madry et al., 2017; Shafahi et al., 2019; Wong et al., 2019; Chen et al., 2022). In addition, recent works Geiping et al. (2021a); Gao et al. (2022) also leverage adversarial training to defend against data poisoning (Huang et al., 2020; Geiping et al., 2021b) and backdoor attacks (Saha et al., 2020; Gu et al., 2019). In general, adversarial training solves a bi-level (min-max) optimization problem. In our work, we formulate RoCourseNet’s objective as a tri-level (min-max-min) optimization problem, which we can decompose into a game played between a model designer and a worst-case (hypothetical) adversary. The inner worst-case data and model shifts are assumed to be generated by a bi-level worst-case attacker. The defender trains a robust CF generator against this bi-level attacker by following an adversarial training procedure.

### 3 Preliminaries

We now discuss the counterfactual explanation (or recourse) problem, and describe the CounterNet architecture Guo et al. (2021), which we use as a building block for RoCourseNet. For ease of exposition, we focus on binary classification problems, but our techniques can be adapted to multi-class settings<sup>2</sup>. Note that we use  $\mathcal{L}(\cdot, \cdot)$  to represent the mean squared error (MSE) loss function (following (Guo et al., 2021)).

**Counterfactual Explanations.** Given an input instance  $x$  and an ML model  $f(\cdot; \theta)$  as input, a counterfactual explanation method finds a CF example (or recourse)  $x^{\text{cf}}$  which receives an opposite prediction from the ML model (i.e.,  $f(x^{\text{cf}}; \theta) = 1 - f(x; \theta)$ ), while ensuring a low cost of change (i.e., the “distance” between  $x$  and  $x^{\text{cf}}$  is low). Let  $c(x, x^{\text{cf}})$  denote the cost of change (e.g.,  $L_1$ -norm distance function) from  $x$  to  $x^{\text{cf}}$ .

<sup>2</sup>See appendix for detailed discussions about extensions to multi-class settings.

Then, most prior techniques (Wachter et al., 2017; Mothilal et al., 2020; Ustun et al., 2019) generate CF explanations  $x^{\text{cf}}$  by solving the following optimization problem separately for each input instance  $x$ :

$$x^{\text{cf}} = \operatorname{argmin}_{x^{\text{cf}}} \mathcal{L}\left(f(x^{\text{cf}}; \theta), 1 - f(x; \theta)\right) + \lambda \cdot c(x, x^{\text{cf}}) \quad (1)$$

The first part of Eq. 1 maximizes the validity to ensure that the generated recourse  $x^{\text{cf}}$  gets an opposite prediction to  $x$ . The second part of Eq. 1 minimizes the cost of change (or distance) between  $x$  and  $x^{\text{cf}}$ . Finally,  $\lambda$  balances the trades-off between the two objective terms.

**CounterNet.** Unlike post-hoc methods described above (Eq. 1), CounterNet (Guo et al., 2021) is an end-to-end framework which combines predictive model training and counterfactual explanation generation into a single optimization pipeline. At a high level, given an instance  $x$  as input, CounterNet produces two outputs: (i) the predictive label  $f(x; \theta_f)$  of the input instance  $x$ , where  $\theta_f = \{\theta_h, \theta_m\}$  in Figure 1; and (ii) the corresponding recourse  $x^{\text{cf}}$  for instance  $x$ . CounterNet has three learning objectives:

$$\operatorname{argmin}_{\theta=\{\theta_f, \theta_g\}} \mathbb{E}_{(x, y) \sim D} \left[ \underbrace{\lambda_1 \cdot \mathcal{L}\left(y, f(x; \theta_f)\right)}_{\text{Prediction Loss } (L_1)} + \underbrace{\lambda_2 \cdot \mathcal{L}\left(f(x^{\text{cf}}; \theta_f), 1 - f(x; \theta_f)\right)}_{\text{Validity Loss } (L_2)} + \underbrace{\lambda_3 \cdot \mathcal{L}\left(x, x^{\text{cf}}\right)}_{\text{Proximity Loss } (L_3)} \right] \quad (2)$$

where  $(\lambda_1, \lambda_2, \lambda_3)$  balance the three loss components. The prediction loss  $L_1$  maximizes predictive accuracy. Similarly, the validity loss  $L_2$  maximizes validity by ensuring that predictions on  $x^{\text{cf}}$  and  $x$  differs. Finally, the proximity loss  $L_3$  minimizes the cost of change required to go from  $x$  to  $x^{\text{cf}}$ .

To optimize Eq. 2, Guo et al. (2021) proposed a block-wise coordinate descent approach. Specifically, for each mini-batch, CounterNet’s parameters are updated twice: it first computes  $\theta' = \theta - \nabla_{\theta}(\lambda_1 \cdot L_1)$ , and for the second update, it computes  $\theta'' = \theta' - \nabla_{\theta'}(\lambda_2 \cdot L_2 + \lambda_3 \cdot L_3)$  (in Eq 2). This coordinate descent procedure ensures that CounterNet achieves state-of-the-art results on static datasets.

Unfortunately, despite promising performance on static datasets, CounterNet is not explicitly designed for scenarios where the predictive models get updated due to shifts in the data distribution. As our experimental evaluation suggests, CounterNet’s validity score degrades by  $\sim 25\%$  when the predictive model is updated with new available data (see Section 5), which reveals the limitations of CounterNet as it fails to generate CF examples robust to model shifts. In this paper, we propose an approach built upon CounterNet, which optimizes for robust recourse generation against data shifts.

## 4 RoCourseNet: A Robust Approach to End-to-End Recourse Generation

RoCourseNet is an end-to-end recourse generation framework that jointly optimizes the generation of accurate predictions and corresponding robust CF examples as part of a single end-to-end pipeline, which is built on top of CounterNet’s architecture (Guo et al., 2021), and also adopts a block-wise coordinate descent procedure for training. However, unlike CounterNet (which does not optimize for robust recourses), RoCourseNet leverages adversarial training to ensure that the CF generator network (Figure 1) produces *robust* CF examples that maintain their validity under model shifts (induced by data shifts), such that  $x^{\text{cf}}$  is a robust CF example for input instance  $x$  iff  $f(x^{\text{cf}}; \theta'_f) = f(x^{\text{cf}}; \theta_f) = 1 - f(x; \theta_f)$ , where  $\theta_f$  and  $\theta'_f$  represent the parameters of original and shifted models, respectively.

At a high level, RoCourseNet’s adversarial training algorithm optimizes a robust CF generator by first constructing a worst-case model shift  $f' \in \mathcal{F}$ , and then optimizes the CF generator such that it generates CF examples  $x^{\text{cf}}$  which remain valid on the shifted model  $f' \in \mathcal{F}$ . Unlike prior work Upadhyay et al. (2021), the worst-case model shift is derived from an explicit data shift which perturbs the input instances (e.g.,  $x_{\text{shift}} = x + \delta$ ). This two-step procedure ensures that the trained CF generator produces CF examples which are highly robust to data shifts. Next, we elaborate on our algorithmic design.

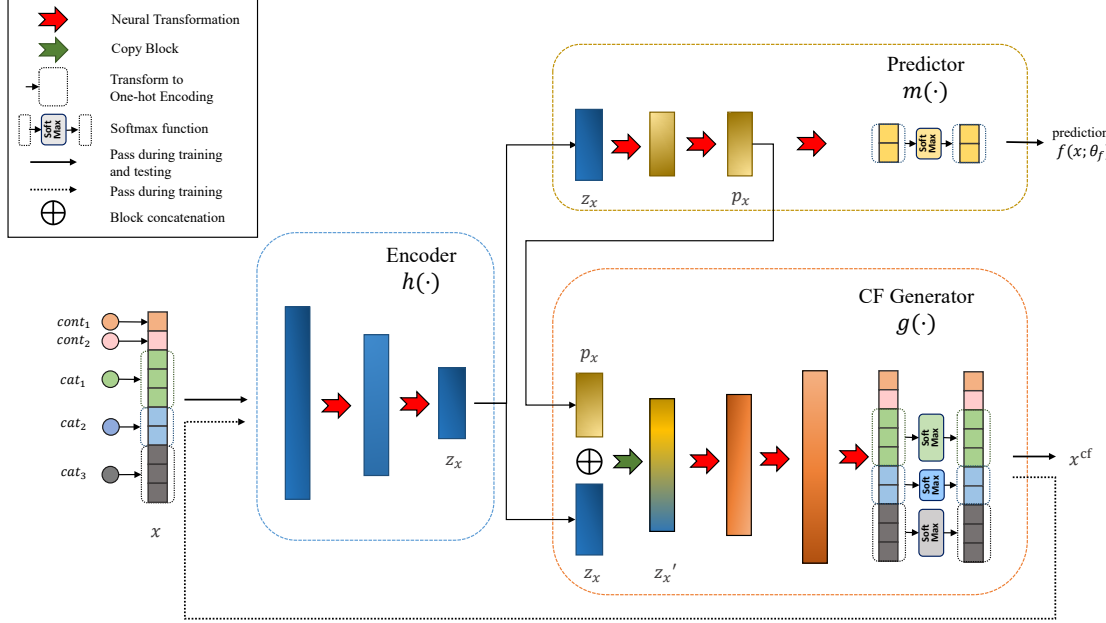


Figure 1: The architecture of CounterNet, the building block of RoCourseNet (Guo et al. (2021)).

#### 4.1 Virtual Data Shift: An Algorithm for Constructing Worst-case Model Shifts

To train a robust CF generator, it is natural to optimize against an adversary who creates a worst-case shifted model (denoted by its weights  $\theta'_f$ ) which can invalidate CF examples (i.e.,  $f(x^{\text{cf}}; \theta'_f) \neq 1 - f(x; \theta_f)$ ). As such, we can find an adversarial shifted model by maximizing the validity loss.

$$\text{argmax}_{\theta'_f \in \mathcal{F}} \mathbb{E}_{(x,y) \sim D} \left[ \mathcal{L} \left( f(x^{\text{cf}}; \theta'_f), 1 - f(x; \theta_f) \right) \right] \quad (3)$$

where  $f(\cdot; \theta_f)$  denotes a predictive model,  $\theta_f$  and  $\theta'_f$  denote the parameters in the original and shifted predictive model (respectively),  $x^{\text{cf}}$  is a CF example produced by the CF generator  $g(\cdot, \theta_g)$  (Figure 1), and  $\mathcal{F} = \{\theta'_f \mid \theta_f + \delta_f\}$  denotes a plausible set of the parameters of all possible shifted models.

However, it is non-trivial to construct a plausible model set  $\mathcal{F}$  by directly perturbing the ML model's parameters, especially when  $f(\cdot; \theta_f)$  is a neural network. Unlike a linear model, quantifying the importance of neurons is challenging (Leino et al., 2018; Dhamdhere et al., 2018), which leads to difficulty in applying weight perturbations. To overcome these challenges, prior work (Upadhyay et al., 2021) adopts a simplified linear model (generated via LIME (Ribeiro et al., 2016)) to approximate the target model, and perturbs this linear model accordingly. Unfortunately, this simplified local linear model introduces approximation errors into the system, which leads to poor performance (as shown in Section 5). Instead, rather than directly perturbing the model's weights, we explicitly consider a worst-case data shift, which originates an adversarial model shift.

**Data shift as a bilevel optimization problem.** We begin by identifying the data shift as the fundamental cause of non-robust CF explanations. In response to a shift in the data distribution (from  $\mathcal{D}$  to  $\mathcal{D}_{\text{shifted}}$ ), the predictive model will get updated by optimizing the prediction loss:

$$\theta'_f(\mathcal{D}_{\text{shifted}})^* = \text{argmin}_{\theta'_f} \mathbb{E}_{(x,y) \sim \mathcal{D}_{\text{shifted}}} \left[ \mathcal{L} \left( f(x; \theta'_f), y \right) \right]. \quad (4)$$

Importantly, this updated predictive model  $f(\cdot, \theta'_f)$  (caused by the shifted data  $\mathcal{D}_{\text{shifted}}$ ) is the key reason which leads to the invalidation of CF examples (i.e.,  $f(x^{\text{cf}}; \theta'_f) \neq 1 - f(x; \theta_f)$ ). Therefore, in order to train a robust CF generator, we optimize against a (hypothetical) adversary who creates a worst-case shifted data distribution  $\mathcal{D}_{\text{shifted}}^*$ , such that the correspondingly updated model (found by solving Equation 4) minimizes the validity score of CF examples  $x^{\text{cf}}$ . Formally, this data shift problem can be formulated as the following bi-level optimization problem:

$$\begin{aligned} & \max_{\delta, \forall \delta \in \Delta} \mathbb{E}_{(x,y) \sim \mathcal{D}} \left[ \mathcal{L} \left( f(x^{\text{cf}}; \theta'_f(\delta)^*), 1 - f(x; \theta_f) \right) \right] \\ & \text{s.t., } \theta'_f(\delta)^* = \operatorname{argmin}_{\theta'_f} \mathbb{E}_{(x,y) \sim \mathcal{D}} \left[ \mathcal{L} \left( f(x + \delta; \theta'_f), y \right) \right]. \end{aligned} \quad (5)$$

where  $\delta \in \Delta$  denotes the data shift for a single data point, and  $\delta = \{\delta_i \mid \forall (x_i, y_i) \in \mathcal{D}\}$  denotes the data shift of each data point in the entire dataset. We define  $\Delta$  as the  $l_\infty$ -norm ball  $\Delta = \{\delta \in \mathbb{R}^n \mid \|\delta\|_\infty \leq \epsilon\}$  (see  $l_2$ -norm in Appendix), which creates a worst-case shifted data  $\mathcal{D}_{\text{shifted}} = \{(x_i + \delta_i, y_i) \mid \delta_i \in \Delta, \forall (x_i, y_i) \in \mathcal{D}\}$ . The outer problem maximizes the validity loss to construct worst-case data shift, and the inner problem learns a shifted model  $\theta'_f$  on the shifted dataset  $\mathcal{D}_{\text{shifted}}$ .

**Virtual Data Shift (VDS) Algorithm.** Unfortunately, solving the bi-level optimization problem in Eq. 5 is computationally intractable due to its nested structure. To approximate this bi-level problem, we devise the *Virtual Data Shift (VDS)* algorithm (shown in Algorithm 1), a gradient based algorithm with an unrolling optimization pipeline. At a high level, VDS iteratively approximates the inner problem via unrolling  $K$ -steps of gradient descent for each outer optimization step. Similar unrolling optimization pipelines are commonly adopted in many ML problems with a bi-level formulation (Shaban et al., 2019; Gu et al., 2022) (e.g., meta-learning (Finn et al., 2017), hyperparameter search (Maclaurin et al., 2015), and poisoning attack (Huang et al., 2020)).

Algorithm 1 layouts the *VDS* algorithm which outputs the worst-case data shifts  $\delta$ , and the corresponding shifted model  $\theta'_f$ . Notably, VDS makes two design choices. First, it uniformly randomizes the data shift  $\delta \sim \mathcal{U}(-\epsilon, +\epsilon)$  (Line 3), following practices of Wong et al. (2019). Uniform randomization is critical to the adversarial model performance as it increases the smoothness of the objective function, leading to improved convergence of gradient-based algorithms (Chen et al., 2022). Then, we iteratively solve this bi-level optimization problem via  $T$  outer attack steps. At each step, we first update the predictor  $\theta'_f$  using the shifted data  $x + \delta$  via  $K$  unrolling steps of gradient descent (Line 6). Next, similar to the fast sign gradient method (FSGM) (Goodfellow et al., 2014), we maximize the adversarial loss and project  $\delta$  into the feasible region  $\Delta$  (i.e.,  $l_\infty$  norm ball; Line 8-9). Crucially, when calculating the gradient of adversarial loss (outer problem) with respect to data shift  $\delta$  (Line 8), we look ahead the inner problem for a few forward steps and then back-propagate to the initial unrolling step. We do this because we use  $K$  unrolling steps of gradient descent, as opposed to full-blown gradient descent till convergence.

In our experiment, we use  $K = 2$  unrolling steps (same as (Huang et al., 2020)) with the step size  $\alpha = 2.5 \times \epsilon/T$  (based on (Madry et al., 2017)). The unrolling learning rate  $\eta$  is the same in training RoCourseNet (see Appendix).

## 4.2 Block-wise Coordinate Descent with Adversarial Training

We now describe RoCourseNet’s training procedure. At a high level, RoCourseNet has three objectives: (i) high *predictive accuracy* - we expect RoCourseNet to output accurate predictions; (ii) high *robust validity* - we expect that generated CF examples in RoCourseNet are valid on shifted models; note that robust validity also ensures validity on the original predictive model (i.e.,  $f(x; \theta_f) = 1 - f(x^{\text{cf}}; \theta_f)$ ), as the worst-case

---

**Algorithm 1** Virtual Data Shift (VDS)

---

- 1: **Hyperparameters:** learning rates  $\eta$ , step size  $\alpha$ , # of attacker steps  $T$ , # of unrolling steps  $K$
- 2: **Input:** model weights  $\theta_f$ , perturbation constraints  $\epsilon$ , minibatch  $(x, y) \in B$ , CF examples  $x^{\text{cf}}$
- 3: **Initialize:** virtual shifted model weights  $\theta'_f = \theta_f$ ,  $\delta \sim \mathcal{U}(-\epsilon, +\epsilon)$
- 4: **for**  $i = 1 \rightarrow T$  steps **do**
- 5:     **for**  $k = 1 \rightarrow K$  unroll steps **do**
- 6:          $\theta'_f = \theta'_f - \eta \cdot \nabla_{\theta'_f} \mathcal{L}(f(x + \delta; \theta'_f), y)$
- 7:     **end for**
- 8:      $\delta = \delta + \alpha \cdot \text{sign}(\nabla_{\delta} \mathcal{L}(f(x^{\text{cf}}; \theta'_f), 1 - f(x; \theta_f)))$
- 9:     Project  $\delta$  onto the feasible region ( $\Delta = \{\delta \in \mathbb{R}^n \mid \|\delta\|_{\infty} \leq \epsilon\}$ ).
- 10: **end for**
- 11: **return**  $\theta'_f, \delta$

---

model shift case encompasses the unshifted model case; (iii) low *proximity* - we desire minimal changes required to modify input instance  $x$  to CF example  $x^{\text{cf}}$ . Based on these objectives, we can formulate the following min-max-min optimization problem:

$$\begin{aligned}
 & \underset{\theta = \{\theta_h, \theta_m, \theta_g\}}{\operatorname{argmin}} \mathbb{E}_{(x, y) \sim D} \left[ \underbrace{\lambda_1 \cdot \mathcal{L}(f(x; \theta_f), y)}_{\text{Prediction Loss } (L_1)} + \lambda_3 \cdot \underbrace{\mathcal{L}(x, x^{\text{cf}})}_{\text{Proximity Loss } (L_3)} \right] \\
 & + \max_{\delta, \forall \delta \in \Delta} \mathbb{E}_{(x, y) \sim D} \left[ \underbrace{\lambda_2 \cdot \mathcal{L}(f(x^{\text{cf}}; \theta'_f(\delta)^*), 1 - f(x; \theta_f))}_{\text{Robust Validity Loss } (L_2)} \right] \quad (6) \\
 & \text{s.t. } \theta'_f(\delta)^* = \operatorname{argmin}_{\theta'_f} \mathbb{E}_{(x, y) \sim D} \left[ \mathcal{L}(f(x + \delta; \theta'_f), y) \right].
 \end{aligned}$$

A common practice in solving a min-max formulation is to first solve the inner maximization problem, and then solve the outer minimization problem (Madry et al., 2017). Therefore, we solve the optimization problem in Eq. 6 as follows (see Algorithm 2): (i) To solve the inner bi-level problem, we find the worst-case model shift by solving Eq. 5 using VDS (Algorithm 1). (ii) To solve the outer minimization problem, we adopt block-wise coordinate descent optimization by distributing gradient descent backpropagation on the objective function into two stages (as suggested in (Guo et al., 2021)) – at stage one, we optimize for predictive accuracy (i.e.,  $L_1$  in Eq. 6), and at stage two, optimize the quality of CF explanations (i.e.,  $\lambda_2 \cdot L_2 + \lambda_3 \cdot L_3$  in Eq. 6).

This block-wise coordinate descent algorithm efficiently optimizes for the outer minimization problem by alleviating the divergent gradient issue, i.e., the gradient directions of prediction loss ( $L_1$ ) and validity loss ( $L_2$ ) moves in different directions, which leads to poor convergence of solving the outer minimization problem as-is via gradient descent (proven in Guo et al. (2021)).

In addition, we linearly increase the perturbation constraints  $\epsilon$  for improved convergence of the training of our robust CF generator. Intuitively, linearly increasing the  $\epsilon$  value corresponds to an increase in the strength of our hypothetical adversary (empirically shown in Section 5). Prior works in curriculum adversarial training (Cai et al., 2018; Wang et al., 2019) suggest that adaptively adjusting the strength of the adversary improves the convergence of adversarial training. Empirically, we observe that adopting curriculum adversarial training boosts the performance of adversarial training (see Section 5).

## 5 Experimental Evaluation

**Baselines.** To the best of our knowledge, RoCourseNet is the first method which optimizes for an end-to-end model for generating predictions and robust CF explanations under distributional data shifts. We compare our method with three state-of-the-art baseline methods. (i) The most relevant baseline method is *Roar-LIME* (Upadhyay et al., 2021). This post-hoc method generates robust CF explanations by optimizing against the worst-case (linear) model shift. (ii) In addition, we experiment with *CounterNet* (Guo et al., 2021), which is the model that RoCourseNet builds upon. *CounterNet* trains an end-to-end model to simultaneously generate predictions and CF explanations. (iii) Finally, we experiment with *VanillaCF* (Wachter et al., 2017), a popular post-hoc method which optimizes validity and proximity of CF explanations (Eq. 1).

Note that other than *CounterNet*, both *VanillaCF* and *ROAR-LIME* require a trained predictive model as an input. Therefore, we train a neural network model that contains only the encoder and predictor inside RoCourseNet (Figure 1), and use it as the base predictive model for these two baselines. For each dataset, we separately tune hyperparameters using grid search (see Appendix for details).

**Datasets.** We evaluate RoCourseNet and baselines on three real-world datasets. (i) We primarily evaluate on the large-sized *Loan Application* dataset (Li et al., 2018) which captures the *temporal shifts* in loan application records. It predicts whether a business defaulted on a loan ( $Y=1$ ) or not ( $Y=0$ ). This large-sized dataset consists of 449,152 loan approval records across U.S. during the years 1994 to 2009 (i.e.,  $\mathcal{D}_{\text{all}} = \{\mathcal{D}_1, \mathcal{D}_2, \dots, \mathcal{D}_k\}$ , where each subset  $\mathcal{D}_i$  corresponds to a particular year, and  $k = 16$  is the total number of years). We adopt Random forests (Breiman, 2001) to select the 12 most predictive features, including 7 continuous and 5 categorical features. (ii) We use the *German Credit* dataset (Asuncion and Newman, 2007), which captures data correction shifts. It predicts whether the credit score of a customer is good ( $Y=1$ ) or bad ( $Y=0$ ). This dataset has 2,000 data points with two versions; each version contains 1,000 data points (i.e.,  $\mathcal{D}_{\text{all}} = \{\mathcal{D}_1, \mathcal{D}_2\}$ , where  $\mathcal{D}_1, \mathcal{D}_2$  corresponds to the original and corrected datasets, respectively). It contains 6 continuous and 3 categorical features. (iii) Finally, we use the *Student* dataset (Cortez and Silva, 2008), which captures geospatial shifts. It predicts whether a student will pass ( $Y=1$ ) or fail ( $Y=0$ ) the final exam. It contains 649 student records in two locations (i.e.,  $\mathcal{D}_{\text{all}} = \{\mathcal{D}_1, \mathcal{D}_2\}$ , where each subset  $\mathcal{D}_i$  corresponds to a particular location). It contains 2 continuous and 14 categorical features.

**Evaluation Procedure & Metrics.** Each evaluated dataset is partitioned into  $k$  subsets  $\mathcal{D}_{\text{all}} = \{\mathcal{D}_1, \mathcal{D}_2, \dots, \mathcal{D}_k\}$ . This partitioning enables us to create  $k$  original datasets  $\mathcal{D}_i \in \mathcal{D}_{\text{all}}$ , and  $k$  corresponding shifted datasets,  $\mathcal{D}_{\text{shifted},i} = \mathcal{D}_{\text{all}} \setminus \mathcal{D}_i$ , where each shifted dataset  $\mathcal{D}_{\text{shifted},i}$  contains all subsets of the dataset  $\mathcal{D}_{\text{all}}$  except for the original dataset  $\mathcal{D}_i$ . Next, each  $\mathcal{D}_i \in \mathcal{D}_{\text{all}}$  is split into a train set and a hold-out test set (i.e.,  $\mathcal{D}_i = \{\mathcal{D}_i^{\text{train}}, \mathcal{D}_i^{\text{test}}\}$ ). We train a separate model (i.e., the entire models for *RoCourseNet* and *CounterNet*, and predictive models for *VanillaCF* and *ROAR-LIME*) on each train set  $\mathcal{D}_i^{\text{train}} \forall i \in \{1, \dots, k\}$ . Then, we use the model trained on  $\mathcal{D}_i^{\text{train}}$  to generate CF examples on the hold-out sets  $\mathcal{D}_i^{\text{test}} \forall i \in \{1, \dots, k\}$ . Finally, we evaluate the robustness (against the model shift) of CF examples generated on  $\mathcal{D}_i^{\text{test}} \forall i \in \{1, \dots, k\}$  as follows: for each CF example  $x^{\text{cf}}$  (corresponding to an input instance  $x$  in  $\mathcal{D}_i^{\text{test}}$ ), we evaluate its robust validity by measuring the fraction of shifted models (i.e.,  $k - 1$  models trained on all shifted training sets) on which  $x^{\text{cf}}$  remains valid.

Finally, we use three metrics to evaluate a CF explanation: (i) *Validity* is defined as the fraction of valid CF examples on the original model  $\theta_f$ . (ii) *Robust validity* is defined as the fraction of valid CF examples on a *shifted* predictive model  $\theta'_f$ . We calculate the robust validity on all possible shifted models. (iii) *Proximity* is defined as the  $l_1$  distance between the input and the CF example. We report the aggregated results of each subset over the entire dataset (see Table 1).

Table 1: Evaluating robustness under model shift for Counterfactual Explanations

Datasets	Metrics	Methods			
		VanillaCF	CounterNet	ROAR-LIME	RoCourseNet
Loan	Proximity	$7.39 \pm 1.860$	<b><math>6.746 \pm 0.723</math></b>	$7.648 \pm 2.248$	$7.183 \pm 0.406$
	Validity	$0.942 \pm 0.026$	$0.964 \pm 0.085$	$0.937 \pm 0.046$	<b><math>0.994 \pm 0.002</math></b>
	Rob-Validity	$0.885 \pm 0.121$	$0.639 \pm 0.222$	$0.908 \pm 0.107$	<b><math>0.930 \pm 0.152</math></b>
German Credit	Proximity	<b><math>4.635 \pm 0.197</math></b>	$5.719 \pm 0.130$	$4.862 \pm 0.117$	$7.075 \pm 0.250$
	Validity	$0.940 \pm 0.011$	$0.960 \pm 0.028$	$0.910 \pm 0.0255$	<b><math>0.986 \pm 0.014</math></b>
	Rob-Validity	$0.772 \pm 0.008$	$0.706 \pm 0.074$	$0.792 \pm 0.052$	<b><math>0.910 \pm 0.034</math></b>
Student	Proximity	$15.236 \pm 0.383$	$18.619 \pm 0.131$	<b><math>11.931 \pm 1.396</math></b>	$21.308 \pm 0.893$
	Validity	$0.915 \pm 0.056$	$0.967 \pm 0.033$	$0.967 \pm 0.026$	<b><math>0.991 \pm 0.009</math></b>
	Rob-Validity	$0.673 \pm 0.006$	$0.859 \pm 0.071$	$0.820 \pm 0.075$	<b><math>0.949 \pm 0.016</math></b>

## 5.1 Experimental Results

**Validity & Robust Validity.** Table 1 compares the validity and robust validity of CF examples generated by RoCourseNet and other baselines on three datasets. This table shows that RoCourseNet outperforms all baselines in terms of both validity and robust validity. In particular, RoCourseNet consistently generates CF examples with 91% robust validity, which shows that the adversarially trained RoCourseNet generates highly robust CF examples when the underlying predictive model shift occurs. Moreover, RoCourseNet achieves  $\sim 10\%$  higher robust validity than Roar-LIME (which optimizes for worst-case model shifts). This result accentuates the importance of considering the data shift, since failing to consider the impact data shift (such as ROAR-LIME) leads to degraded results.

In addition, RoCourseNet consistently generates CF examples with more than 98.5% validity, which is  $\sim 6\%$ ,  $\sim 5\%$ ,  $\sim 3\%$  higher than VanillaCF, ROAR-LIME, and CounterNet, respectively. This result shows that optimizing the worst-case shifted model (i.e.,  $L_2$  in Eq. 6) is sufficient to achieve high validity, without the need to explicitly optimize for an additional validity loss on the original model.

**Proximity.** Table 1 compares the proximity of CF examples produced by RoCourseNet and baselines on all three datasets. In particular, RoCourseNet performs exceedingly on the Loan application dataset (our largest dataset with  $\sim 450k$  data points), as it is the second-best method in terms of proximity (just behind CounterNet), and outperforms both our post-hoc baseline methods (VanillaCF and Roar-LIME). On the other hand, RoCourseNet achieves  $\sim 40\%$  and  $\sim 90\%$  poorer proximity as compared to the best performing baselines on the German Credit and Student datasets, respectively.

Note that the relatively poorer performance on proximity in *German Credit* and *Student* datasets is attributed to the cost-invalidity trade-off, as a high robust validity (which is the case in RoCourseNet) often comes at the cost of proximity (Rawal et al., 2020). In addition, to balance this trade-off well, sufficient training data is required. Unfortunately, these two small-sized datasets both contain less than 1k data points (in contrast of  $\sim 450k$  data points in the *Loan* dataset), which limit our balancing of the cost-invalidity trade-off. We further illustrate the cost-invalidity trade-off in the next section.

## 5.2 Further Analysis

**Evaluating VDS Attacker.** We first demonstrate the effectiveness of VDS on solving the inner maximization problem in Eq. 6, i.e., how often VDS succeeds in finding an adversarial shifted model  $\theta'_f$ , such that the generated CF examples  $x^{\text{cf}}$  are invalid on that shifted model (i.e.,  $f(x^{\text{cf}}; \theta'_f) \neq 1 - f(x; \theta_f)$ ). To evaluate the performance of VDS, we apply Algorithm 1 to find a shifted model  $\theta'_f$ , and compute the robust validity of all hold-out test-sets with respect to this shifted model.

Figure 2a and 2d illustrate the effectiveness of attacking CounterNet and RoCourseNet via the VDS algorithm, which highlights three important findings: (i) First, the VDS algorithm is effective in solving the bi-level problem in Eq. 5 as it can effectively find a shifted model which invalidates a given CF example  $x^{\text{cf}}$ . In particular, the average robust validity drops to 74.8% when the attacker steps  $T$  is set to 20, as compared to 99.8% validity on the original model. (ii) Moreover, increasing attacker steps  $T$  and the maximum perturbation  $E$  improves the effectiveness of finding a shifted adversarial model. Figure 2a shows that when  $T$  is increased, the robust validity of both CounterNet and RoCourseNet is degraded, which indicates that increasing steps improves the effectiveness of solving the bi-level problem in Eq. 5. Similarly, Figure 2d shows that increasing  $E$  also improves effectiveness of solving Eq. 5. (iii) Finally, RoCourseNet is more robust than CounterNet when attacked by the VDS algorithm, as RoCourseNet vastly outperforms CounterNet in robust validity (e.g.,  $\sim 28\%$ ,  $\sim 10\%$  improved robust validity when  $T = 20$ ,  $E = 0.5$  in Figure 2a and 2d, respectively).

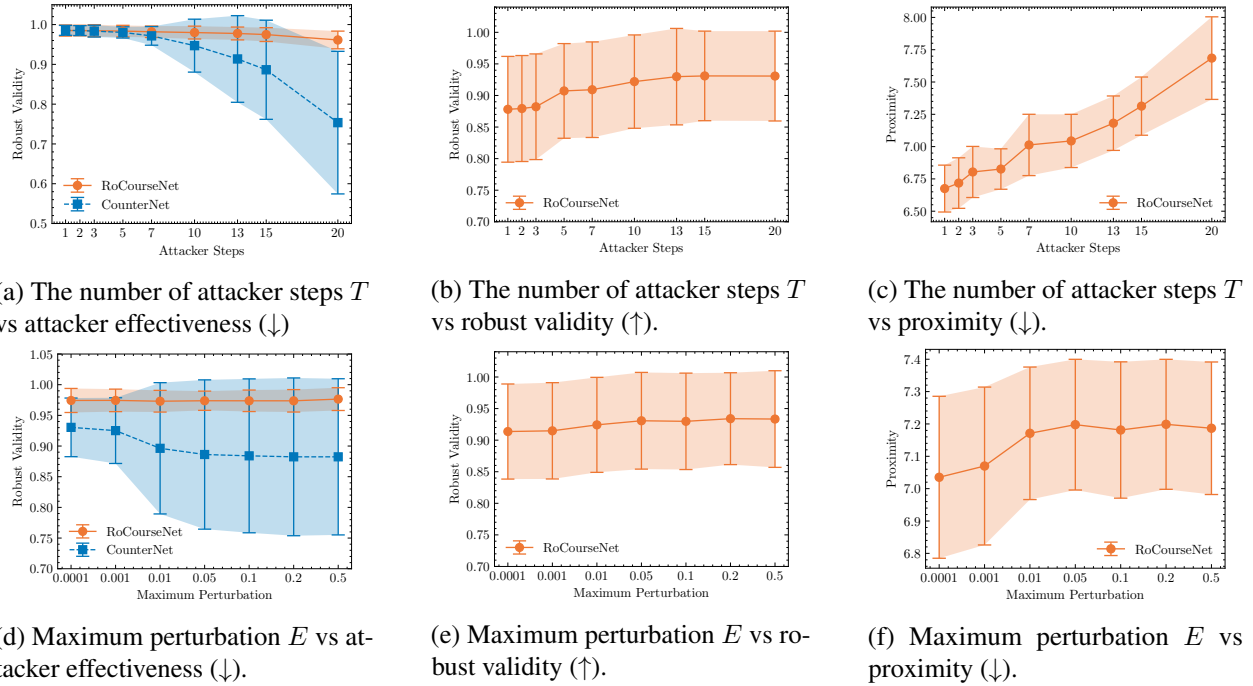


Figure 2: The impact of the number of attacker steps  $T$  (2a-2c) and max-perturbation  $E$  (2d-2f) to robustness on the *Loan* dataset ( $\uparrow$  or  $\downarrow$  means that higher or lower value is preferable, respectively). (i) 2a and 2d depict the role of  $T$  (when  $E = 0.1$ ) and  $E$  (when  $T = 15$ ) in the attacker settings, respectively. (ii) 2b, 2c and 2e, 2f describe the role of  $T$  and  $E$  in the defense setting, respectively.

**Understanding the Tri-level Robust CF Training.** We provide further analysis about our tri-level robust training procedure. First, we observe that a stronger attacker (i.e., more effective in solving Eq. 5) contributes to the training of a more robust CF generator. In Figure 2b, we observe that increasing  $T$  (which results

in a stronger attacker as shown in Figure 2a) leads to improved robust validity, which indicates a more robust CF generator. Similarly, Figure 2e illustrates that increasing  $E$  values leads to improved robustness of counterfactual validity. These results show that having an appropriately strong attacker (i.e., effectively optimizing Eq. 5) is crucial to train for a robust CF generator.

**COST-INVALIDITY TRADE-OFF.** In addition, we analyze the trade-off between cost of change (i.e., proximity) and the invalidation percentage (defined as  $1 - \text{validity}$ ) (Rawal et al., 2020). Conceptually, to ensure the validity of CF explanations, the cost will naturally increase (otherwise, the CF example  $x^{\text{cf}}$  could be naively set to input instance  $x$  itself, which has low proximity, but high invalidity). Furthermore, to achieve high robust validity, we need to further sacrifice proximity. Figure 2 highlights this cost-invalidity trade-off. In particular, this figure shows that increasing the robust validity (shown in both Figure 2b and 2e) comes with the cost of increased proximity.

**EPSILON SCHEDULER.** Finally, we illustrate the importance of linearly scheduling  $\epsilon$  values inside VDS (see Appendix for experiments with non-linear scheduling). Figure 3 shows the effectiveness of adopting this curriculum training procedure. By linearly increasing the epsilons, we observe  $\sim 0.88\%$  improved robust validity (on average) compared to using a static epsilon  $E$  during the entire adversarial training. This result shows that this curriculum training strategy can boost the robustness of CF examples.

## 6 Limitations & Conclusion

**Limitations and Future Work.** Our work has two limitations that future studies should address. (i) We primarily consider the covariate shift scenario, whereas other types of distributional shifts (e.g., label shift, concept shift) might also occur in the real-world. (ii) One must be aware of the potential negative social impact as RoCourseNet might amplify pre-existing societal biases to end-users. A short-term workaround is to have human-in-the-loop by having human operators communicate the CF explanations respectfully. In the long term, further quantitative and qualitative studies are needed to understand the social impact of RoCourseNet.

**Conclusion.** This paper presents *RoCourseNet*, an end-to-end training framework to generate predictions and robust CF explanations against data shifts. We formulate this robust end-to-end training as a min-max-min optimization problem, and leverage adversarial training to effectively solve this complicated tri-level problem. Empirical results show that RoCourseNet outperforms state-of-the-art baselines in robust validity with well-balanced cost-invalidity trade-off.

## References

Asuncion, A. and Newman, D. (2007). Uci machine learning repository.

Barocas, S., Selbst, A. D., and Raghavan, M. (2020). The hidden assumptions behind counterfactual explanations and principal reasons. In *Proceedings of the 2020 Conference on Fairness, Accountability, and Transparency*, pages 80–89.

Breiman, L. (2001). Random forests. *Machine learning*, 45(1):5–32.

Cai, Q.-Z., Liu, C., and Song, D. (2018). Curriculum adversarial training. In *Proceedings of the 27th International Joint Conference on Artificial Intelligence*, pages 3740–3747.

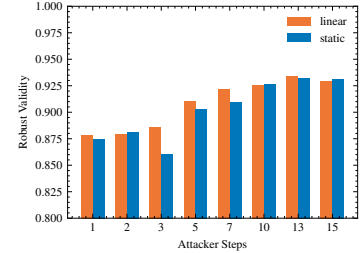


Figure 3: Impact of epsilon scheduler on the robustness.

Chen, J., Cheng, Y., Gan, Z., Gu, Q., and Liu, J. (2022). Efficient robust training via backward smoothing. In *Proceedings of the AAAI Conference on Artificial Intelligence (AAAI)*.

Cortez, P. and Silva, A. M. G. (2008). Using data mining to predict secondary school student performance.

Dhamdhere, K., Sundararajan, M., and Yan, Q. (2018). How important is a neuron? *arXiv preprint arXiv:1805.12233*.

Dhurandhar, A., Chen, P.-Y., Luss, R., Tu, C.-C., Ting, P., Shanmugam, K., and Das, P. (2018). Explanations based on the missing: Towards contrastive explanations with pertinent negatives. In *Proceedings of the 32nd International Conference on Neural Information Processing Systems, NIPS'18*, page 590–601, Red Hook, NY, USA. Curran Associates Inc.

Finn, C., Abbeel, P., and Levine, S. (2017). Model-agnostic meta-learning for fast adaptation of deep networks. In *International conference on machine learning*, pages 1126–1135. PMLR.

Gao, Y., Wu, D., Zhang, J., Gan, G., Xia, S.-T., Niu, G., and Sugiyama, M. (2022). On the effectiveness of adversarial training against backdoor attacks. *arXiv preprint arXiv:2202.10627*.

Geiping, J., Fowl, L., Somepalli, G., Goldblum, M., Moeller, M., and Goldstein, T. (2021a). What doesn't kill you makes you robust (er): Adversarial training against poisons and backdoors. *arXiv preprint arXiv:2102.13624*.

Geiping, J., Fowl, L. H., Huang, W. R., Czaja, W., Taylor, G., Moeller, M., and Goldstein, T. (2021b). Witches' brew: Industrial scale data poisoning via gradient matching. In *International Conference on Learning Representations*.

Goodfellow, I. J., Shlens, J., and Szegedy, C. (2014). Explaining and harnessing adversarial examples. *arXiv preprint arXiv:1412.6572*.

Grefenstette, E., Amos, B., Yarats, D., Htut, P. M., Molchanov, A., Meier, F., Kiela, D., Cho, K., and Chintala, S. (2019). Generalized inner loop meta-learning. *arXiv preprint arXiv:1910.01727*.

Gu, A., Lu, S., Ram, P., and Weng, L. (2022). Min-max bilevel multi-objective optimization with applications in machine learning. *arXiv preprint arXiv:2203.01924*.

Gu, T., Liu, K., Dolan-Gavitt, B., and Garg, S. (2019). Badnets: Evaluating backdooring attacks on deep neural networks. *IEEE Access*, 7:47230–47244.

Guo, H., Nguyen, T., and Yadav, A. (2021). Counternet: End-to-end training of counterfactual aware predictions. In *ICML 2021 Workshop on Algorithmic Recourse*.

Hoofnagle, C. J., van der Sloot, B., and Borgesius, F. Z. (2019). The european union general data protection regulation: what it is and what it means. *Information & Communications Technology Law*, 28(1):65–98.

Huang, W. R., Geiping, J., Fowl, L., Taylor, G., and Goldstein, T. (2020). Metapoison: Practical general-purpose clean-label data poisoning. *Advances in Neural Information Processing Systems*, 33:12080–12091.

Karimi, A.-H., Barthe, G., Schölkopf, B., and Valera, I. (2020). A survey of algorithmic recourse: definitions, formulations, solutions, and prospects. *arXiv preprint arXiv:2010.04050*.

Karimi, A.-H., Schölkopf, B., and Valera, I. (2021). Algorithmic recourse: from counterfactual explanations to interventions. In *Proceedings of the 2021 ACM Conference on Fairness, Accountability, and Transparency*, pages 353–362.

Kim, B., Wattenberg, M., Gilmer, J., Cai, C., Wexler, J., Viegas, F., et al. (2018). Interpretability beyond feature attribution: Quantitative testing with concept activation vectors (tcav). In *International conference on machine learning*, pages 2668–2677. PMLR.

Koh, P. W. and Liang, P. (2017). Understanding black-box predictions via influence functions. In *International conference on machine learning*, pages 1885–1894. PMLR.

Leino, K., Sen, S., Datta, A., Fredrikson, M., and Li, L. (2018). Influence-directed explanations for deep convolutional networks. In *2018 IEEE International Test Conference (ITC)*, pages 1–8. IEEE.

Li, M., Mickel, A., and Taylor, S. (2018). “should this loan be approved or denied?”: A large dataset with class assignment guidelines. *Journal of Statistics Education*, 26(1):55–66.

Lundberg, S. M. and Lee, S.-I. (2017). A unified approach to interpreting model predictions. In *Advances in neural information processing systems*, pages 4765–4774.

Maclaurin, D., Duvenaud, D., and Adams, R. (2015). Gradient-based hyperparameter optimization through reversible learning. In *International conference on machine learning*, pages 2113–2122. PMLR.

Madry, A., Makelov, A., Schmidt, L., Tsipras, D., and Vladu, A. (2017). Towards deep learning models resistant to adversarial attacks. *arXiv preprint arXiv:1706.06083*.

Mahajan, D., Tan, C., and Sharma, A. (2019). Preserving causal constraints in counterfactual explanations for machine learning classifiers. *arXiv preprint arXiv:1912.03277*.

Mothilal, R. K., Sharma, A., and Tan, C. (2020). Explaining machine learning classifiers through diverse counterfactual explanations. In *Proceedings of the 2020 Conference on Fairness, Accountability, and Transparency*, pages 607–617.

Pawelczyk, M., Broelemann, K., and Kasneci, G. (2020a). Learning model-agnostic counterfactual explanations for tabular data. In *Proceedings of The Web Conference 2020*, pages 3126–3132.

Pawelczyk, M., Broelemann, K., and Kasneci, G. (2020b). On counterfactual explanations under predictive multiplicity. In *Conference on Uncertainty in Artificial Intelligence*, pages 809–818. PMLR.

Pawelczyk, M., Datta, T., van-den Heuvel, J., Kasneci, G., and Lakkaraju, H. (2022). Algorithmic recourse in the face of noisy human responses. *arXiv preprint arXiv:2203.06768*.

Rawal, K., Kamar, E., and Lakkaraju, H. (2020). Algorithmic recourse in the wild: Understanding the impact of data and model shifts. *arXiv preprint arXiv:2012.11788*.

Ribeiro, M. T., Singh, S., and Guestrin, C. (2016). ” why should i trust you?” explaining the predictions of any classifier. In *Proceedings of the 22nd ACM SIGKDD international conference on knowledge discovery and data mining*, pages 1135–1144.

Rudin, C. (2019). Stop explaining black box machine learning models for high stakes decisions and use interpretable models instead. *Nature Machine Intelligence*, 1(5):206–215.

Saha, A., Subramanya, A., and Pirsavash, H. (2020). Hidden trigger backdoor attacks. In *Proceedings of the AAAI conference on artificial intelligence*, volume 34, pages 11957–11965.

Shaban, A., Cheng, C.-A., Hatch, N., and Boots, B. (2019). Truncated back-propagation for bilevel optimization. In *The 22nd International Conference on Artificial Intelligence and Statistics*, pages 1723–1732. PMLR.

Shafahi, A., Najibi, M., Ghiasi, M. A., Xu, Z., Dickerson, J., Studer, C., Davis, L. S., Taylor, G., and Goldstein, T. (2019). Adversarial training for free! *Advances in Neural Information Processing Systems*, 32.

Slack, D., Hilgard, S., Jia, E., Singh, S., and Lakkaraju, H. (2020). Fooling lime and shap: Adversarial attacks on post hoc explanation methods. In *Proceedings of the AAAI/ACM Conference on AI, Ethics, and Society*, pages 180–186.

Stepin, I., Alonso, J. M., Catala, A., and Pereira-Fariña, M. (2021). A survey of contrastive and counterfactual explanation generation methods for explainable artificial intelligence. *IEEE Access*, 9:11974–12001.

Upadhyay, S., Joshi, S., and Lakkaraju, H. (2021). Towards robust and reliable algorithmic recourse. *arXiv preprint arXiv:2102.13620*.

Ustun, B., Spangher, A., and Liu, Y. (2019). Actionable recourse in linear classification. In *Proceedings of the Conference on Fairness, Accountability, and Transparency*, pages 10–19.

Van Looveren, A. and Klaise, J. (2019). Interpretable counterfactual explanations guided by prototypes. *arXiv preprint arXiv:1907.02584*.

Verma, S., Dickerson, J., and Hines, K. (2020). Counterfactual explanations for machine learning: A review. *arXiv preprint arXiv:2010.10596*.

Wachter, S., Mittelstadt, B., and Russell, C. (2017). Counterfactual explanations without opening the black box: Automated decisions and the gdpr. *Harv. JL & Tech.*, 31:841.

Wang, Y., Ma, X., Bailey, J., Yi, J., Zhou, B., and Gu, Q. (2019). On the convergence and robustness of adversarial training. In *International Conference on Machine Learning*, pages 6586–6595. PMLR.

Wong, E., Rice, L., and Kolter, J. Z. (2019). Fast is better than free: Revisiting adversarial training. In *International Conference on Learning Representations*.

Yang, F., Alva, S. S., Chen, J., and Hu, X. (2021). Model-based counterfactual synthesizer for interpretation. In *Proceedings of the 27th ACM SIGKDD Conference on Knowledge Discovery and Data Mining*, KDD '21, page 1964–1974, New York, NY, USA. Association for Computing Machinery.

## A Implementation Details

Here we provide implementation details of RoCourseNet and three baseline methods on three datasets listed in Section 5. The code can be found through this anonymous repository ([https://github.com/bkghz-orange-blue/counternet\\_adv](https://github.com/bkghz-orange-blue/counternet_adv)).

**Feature Engineering.** We follow the feature engineering procedure of CounterNet (Guo et al., 2021). Specifically, for continuous features, we scale all feature values into the  $[0, 1]$  range. To handle the categorical features, we customize RoCourseNet’s architecture (in Figure 1) for each dataset. First, we transform the categorical features into numerical representations via one-hot encoding. In addition, for each categorical feature, we add a softmax layer after the final output layer in the CF generator (in Figure 1), which ensures that the generated CF examples respect the one-hot encoding format.

**Hyperparameters.** For all three datasets, we train the model for up to 50 epochs with Adam. We set dropout rate to 0.3 to prevent overfitting. We use  $T = 13$  and  $E = 0.1$  to report results in Table 1, and report the impact of attacker steps  $T$  and maximum perturbation  $E$  to robustness in Figure 2. In addition, Table 2 reports the hyperparameters chosen for each dataset, and Table 3 specifies the architecture used for each dataset.

Table 2: Hyperparameters setting for each dataset.

Dataset	Learning Rate	Batch Size	$\lambda_1$	$\lambda_2$	$\lambda_3$
<b>Loan</b>	0.003	128	1.0	0.2	0.1
<b>German Credit</b>	0.003	256	1.0	1.0	0.1
<b>Student</b>	0.01	128	1.0	0.2	0.1

Table 3: Architecture specification of RoCourseNet for each dataset.

Dataset	Encoder Dims	Predictor Dims	CF Generator Dims
<b>Loan</b>	[110,200,10]	[10, 10]	[10, 10]
<b>German Credit</b>	[19, 100, 10]	[10, 20]	[10, 20]
<b>Student</b>	[83,50,10]	[10, 10]	[10, 50]

**Software and Hardware Specifications.** We use Python (v3.7) with Pytorch (v1.82), Pytorch Lightning (v1.10), numpy (v1.19.3), pandas (v1.1.1), scikit-learn (v0.23.2) and higher (v0.2.1) Grefenstette et al. (2019) for the implementations. All our experiments were run on a Debian-10 Linux-based Deep Learning Image on the Google Cloud Platform. The RoCourseNet and baseline methods are trained (or optimized) on a 16-core Intel machine with 64 GB of RAM.

## B Additional Experimental Analysis

### B.1 Predictive Accuracy

We first show that, similar to CounterNet, the training of RoCourseNet does not come at the cost of degraded predictive accuracy. Table 4 compares RoCourseNet’s predictive accuracy against the base prediction model used by baselines. This table shows that RoCourseNet achieves competitive predictive performance – it achieves marginally better accuracy than the base model ( $\sim 2\%$ ). Thus, we conclude that the joint training of RoCourseNet does not come at a cost of reduced predictive performance.

Table 4: Predictive accuracy for each dataset.

Dataset	Base Model	RoCourseNet
<b>Loan</b>	$0.886 \pm 0.036$	$0.885 \pm 0.035$
<b>German Credit</b>	$0.714 \pm 0.003$	$0.742 \pm 0.014$
<b>Student</b>	$0.914 \pm 0.028$	$0.906 \pm 0.066$

## B.2 $l_2$ -norm Projection in Algorithm 1

We provide supplementary results on adopting  $\Delta$  as the  $l_2$ -norm ball (i.e.,  $\Delta = \{\delta \in \mathbb{R}^n \mid \|\delta\|_2 \leq \epsilon\}$ ) for the maximum perturbation constraints. Figure 4 highlights the results of using the  $l_2$ -norm ball in attacking and adversarial training. We observe similar patterns in Figure 2. Thus, this result shows that  $l_\infty$ -norm constrain can be substitute to other feasible region.

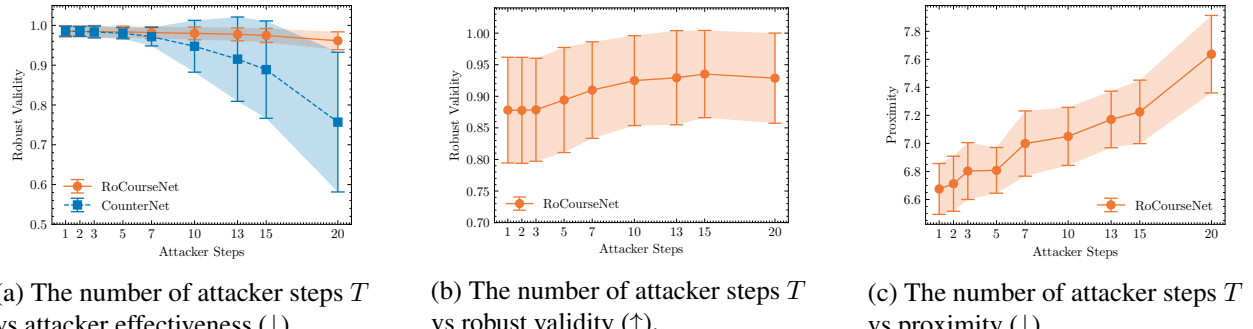


Figure 4: The impact of the number of attacker steps  $T$  under the  $l_2$ -norm constrains.

## C Discussion about Generalized Frameworks to RoCourseNet

This section discusses extending the training of RoCourseNet (see Algorithm 1 & 2) into a broader framework, i.e., we can substitute predictor and CF generator components (in Figure 1) to other parametric models. Crucially, we can extend the RoCourseNet training into a general framework, which contains two components: (i) a predictor  $f(\cdot; \theta_f)$ , which makes an accurate prediction for a given input instance  $x$ , (ii) and a CF generator  $g(\cdot; \theta_g)$ , which generates its corresponding CF explanations. This general framework does not require a shared structure similar to the RoCourseNet architecture (in Figure 1). We can choose separate models for the predictor  $f(\cdot; \theta_f)$  and CF generator  $g(\cdot; \theta_g)$ . In addition, we can train this framework exactly as we train RoCourseNet via Algorithm 2, which optimizes for predictor  $f(\cdot; \theta_f)$  and robust CF generator  $g(\cdot; \theta_g)$ .

**Experimental Settings.** We demonstrate the feasibility of training this general framework (denoted as *Robust CF Framework* in Table 5). For fair comparison, we use the same hyperparameters in training RoCourseNet (See Appendix A) to optimize this general framework. In addition, we use the same architecture specifications of RoCourseNet, as the predictor of this framework combines the encoder network and predictor network in RoCourseNet, and the CF generator network combines the encoder network and CF generator in RoCourseNet.

**Empirical Results.** Table 5 compares this general robust CF framework with RoCourseNet and Roar-LIME. This table highlights two important findings: (i) First, our proposed tri-level robust training (in Algorithm 2) can be extended to a general framework to optimize a robust CF generator. In particular, this robust CF framework outperforms Roar-LIME in terms of proximity and validity, and achieves the same level of robust validity as Roar-LIME. (ii) Additionally, we highlight the importance of RoCourseNet design (by leveraging the design of CounterNet (Guo et al., 2021)). This architecture design enables to generate well-aligned CF

explanations by passing the predictor model’s decision boundary (i.e.,  $p_x$ ) to the CF generator. From Table 5, we observe that RoCourseNet outperforms this Robust CF Framework in terms of the validity and robust validity, which underscores the importance of RoCourseNet’s architecture designs.

Table 5: Evaluating robustness under model shift using a general framework.

Methods	Metrics		
	Proximity	Validity	Rob-Validity
<b>Robust CF Framework</b>	$7.150 \pm 1.078$	$0.949 \pm 0.022$	$0.906 \pm 0.119$
<b>Roar-LIME</b>	$7.648 \pm 2.248$	$0.937 \pm 0.046$	$0.908 \pm 0.107$
<b>RoCourseNet</b>	$7.183 \pm 0.406$	<b><math>0.994 \pm 0.002</math></b>	<b><math>0.930 \pm 0.152</math></b>

## D Discussion about Multi-class Classification

Existing CF explanation literature focuses on evaluating methods under the binary classification settings (Mothilal et al., 2020; Mahajan et al., 2019; Upadhyay et al., 2021; Guo et al., 2021). However, these CF explanation methods can be adapted to the multi-class classification settings. Given an input instance  $x \in \mathbb{R}^d$ , the RoCourseNet generates (i) a prediction  $\hat{y}_x \in \mathbb{R}^k$  for input instance  $x$ , and (ii) a CF example  $x^{\text{cf}}$  as an explanation for input instance  $x$ . The prediction  $\hat{y}_x \in \mathbb{R}^k$  is encoded as one-hot format as  $\hat{y}_x \in \{0, 1\}^k$ , where  $\sum_i \hat{y}_x^{(i)} = 1$ ,  $k$  denotes the number of classes. In addition, we assume a desired outcome  $y'$  for every input instances  $x$ . As such, we can adapt Eq. 6 for binary settings to the multi-class settings as follows:

$$\begin{aligned}
 & \underset{\theta=\{\theta_h, \theta_m, \theta_g\}}{\operatorname{argmin}} \mathbb{E}_{(x, y) \sim D} \left[ \underbrace{\lambda_1 \cdot \mathcal{L}(f(x; \theta_f), y)}_{\text{Prediction Loss } (L_1)} + \lambda_3 \cdot \underbrace{\mathcal{L}(x, x^{\text{cf}})}_{\text{Proximity Loss } (L_3)} \right] \\
 & + \max_{\delta, \forall \delta \in \Delta} \mathbb{E}_{(x, y) \sim D} \left[ \underbrace{\lambda_2 \cdot \mathcal{L}(f(x^{\text{cf}}; \theta'_f(\delta)^*), y')}_{\text{Robust Validity Loss } (L_2)} \right] \\
 & \text{s.t. } \theta'_f(\delta)^* = \operatorname{argmin}_{\theta'_f} \mathbb{E}_{(x, y) \sim D} \left[ \mathcal{L}(f(x + \delta; \theta'_f), y) \right]. \tag{7}
 \end{aligned}$$

To optimize for Eq. 7, we can follow the same procedure outlined in Algorithm 2. For each sampled batch, we first optimize for the predictive accuracy  $\theta' = \theta - \nabla_{\theta}(\lambda_1 \cdot L_1)$ . Next, we use the VDS algorithm to optimize for the inner max-min bi-level problem (in Algorithm 1). Finally, we optimize for the CF explanations by updating the model’s weight as  $\theta''_g = \theta''_g - \nabla_{\theta'_g}(\lambda_2 \cdot L_2 + \lambda_3 \cdot L_3)$ .